

IAC-22-D1.6.6x72833

Design and Integration of a Multi-arm Installation Robot Demonstrator for orbital large Assembly

**Mathieu Deremetz ^{a*}, Maxence Debroise ^a, Marco De Stefano ^b, Hrishik Mishra ^b, Bernhard Brunner ^b,
Gerhard Grunwald ^b, Máximo A. Roa ^b, Matthias Reiner ^b, Martin Závodník ^c, Martin Komarek ^d, Jurij
D'Amico ^e, Francesco Cavenago ^f, Jeremi Gancet ^a, Shashank Govindaraj ^a, Pierre Letier ^a, Michel Ilzkovitz ^a,
Levin Gerdes ^g, Martin Zwick ^g**

^a Space Applications Services NV/SA, Leuvensesteenweg 325, 1932 Sint-Stevens-Woluwe (Brussels Area), Belgium, firstname.lastname@spaceapplications.com

^b Institute of Robotics and Mechatronics, German Aerospace Center (DLR), 82234 Wessling, Germany, firstname.lastname@dlr.de

^c Frentech Aerospace s.r.o., Jarní 977/48, 614 00 Brno-Maloměřice a Obřany, Czech Republic, firstname.lastname@frentech.eu

^d L.K. Engineering s.r.o., Vídeňská 55, 639 00 Brno, Czech Republic, lastname@lke.cz

^e Thales Alenia Space France, 26 Avenue J.F. Champollion, 31037 Toulouse Cedex 1, France firstname.lastname@thalesalieniaspace.com

^f Leonardo S.p.A., Viale Europa, 20014 Nerviano (MI), Italy, firstname.lastname@leonardocompany.com

^g Automation and Robotics Section, European Space Agency (ESA), Keplerlaan 1, 2201 AZ Noordwijk, The Netherlands, firstname.lastname@esa.int

* Corresponding Author

Abstract

Space facilities for orbital exploitation and exploration missions are increasingly requiring larger structure to extend their capabilities. Dimensions of future scientific outposts, solar stations and telescopes undoubtedly matter to expand our horizons, power our planet or explore the universe. Due to the foreseen large structures for such applications, a single self-deploying piece contained in standard launcher fairings might become inadequate. Another approach is that large structures could be broken down into standard modules that will be built in-orbit. Assembling large structure in space is particularly challenging but the raise of key enablers as standard interconnects and advanced robotics opens a new horizon for such applications. It is assumed here that the large spacecraft structure and modules are equipped with standard interconnects (SI) that allow them to be mated to each other and to the robot system for manipulation/transport/installation, or to allow the robot system to move across them.

This paper introduces the concept of a novel Multi-Arm Robot (MAR) dedicated to on-orbit large telescope assembly, its ground equivalent laboratory demonstrator design and preliminary hardware integration.

The MAR is a modular robot composed of three robotic subsystems - a torso and two symmetrical 7-degree of freedom (DOF) anthropomorphic arms with non-spherical wrists - that are functionally independent and can be connected by the means of Standard Interconnects. The modular approach of the MAR reduces the complexity of the different robotic appendages and offers a set of robotic configuration that extends the range of possible operations and provides an intrinsic system redundancy that reduces the overall mission risk.

To assess the MAR concept, a Technology Readiness Level (TRL) 4 ground demonstrator, has been designed to provide a framework that allows the multi-arm robot to execute its overall scope of operations in a ground laboratory environment. It comprises a testbed (dummy spacecraft structure, home base, storage area and mobile payloads) offering a space representative environment, a mission control center (computer, simulator and electrical/data support equipment) supervising the MAR's tasks, and a gravity compensation system (gantry crane and offloading system) for supporting the robot under 1-g.

This study is funded by the European Space Agency (ESA) in the framework of the Technology Research Program (contract No. 4000132220/20/NL/RA) entitled "Multi-arm Installation Robot for Readyng ORUS and Reflectors (MIRROR)".

Keywords: Space robotics, Relocatable robot, Modular robot, Mechanism Design of Manipulators, Standard Interconnects

Acronyms/Abbreviations

Centralized Power Distribution Unit (CPDU), Electrical Ground Support Equipment (EGSE), International Space Station (ISS), Monitoring and Control Center (MCC), On-Board Computer (OBC), Orbital replacement unit (ORU), Operating System (OS), Servo Control Unit (SCU), Task Oriented Programming (TOP).

1. Introduction

Large structures in space are an essential and recurring element for space exploitation and exploration. Future outposts, solar facilities, and telescope sizes will undoubtedly drive the space capabilities [1]. While self-deploying structures contained in typical launcher fairings becomes less appropriate because of the growing size of foreseen structures, large structures divided into modules and further assembled in space may appear as the preferred implementation approach [2]. In-space assembly (IAS) of large structure is extremely challenging, but technologies like standard interconnects and dexterous orbital robotics open new opportunities for such applications [1-3].

In the context of the ESA "Multi-arm Installation Robot for Readyng ORUS and Reflectors (MIRROR)" project, this paper introduces the concept of a novel Multi-Arm Robot dedicated to on-orbit large telescope assembly (see Fig. 1), its ground equivalent laboratory demonstrator design, and preliminary breadboard integration.



Figure 1. Artist representation of the MAR concept.

Here, the large spacecraft structure, modules and installation robot are assumed to be equipped with HOTDOCK Standard Interconnects that enable mechanical, data, and power transfer [4]. Thus, modules can mate with each other, robotic manipulators can

capture, transport and install them, and the installation robot can relocate over the spacecraft structure and modules.

This work leverages results, concepts or ideas from a number of previous European projects: H2020 Space Robotics projects (ESROCOS [5], SIROM [6], PULSAR [7] and MOSAR [8, 9]), ESA ISS EUROBOT project [10], ESA TRP Dexterous Robot Arm (DEXARM) [11] and standard interconnects [4].

The structure of this paper is as follows: Sec. 2 recalls MIRROR's mission scenario and concept of operations and Sec. 3 follows with the introduction of the ground technological demonstrator. Sec. 4 presents the breadboard detailed design, while Sec. 5 illustrated its preliminary hardware integration. Sec. 6 finally provides a conclusion on the work achieved and presents perspectives on future activities.

2. Mission scenario and concept of operations

MIRROR is a robotic system which provide self-assembly and self-maintenance capabilities to a satellite. In this scenario, a hosting spacecraft located in the Sun-Earth Lagrangian point is assumed, acting also as a logistic node for additional servicing operations. As a baseline, the hypothesis is to have a multi arm robot stowed in the satellite at his home base attached to the satellite primary structure by means of standard interconnects [4]. The spacecraft includes a service module, a payload module and a dispenser storing the individual mirror tiles. Fig. 2 shows the assumed multi arm robot stowed configuration in the Ariane-6 satellite during the launch phase.

Once the spacecraft has reached the Sun-Earth L2 point, the assembly sequence is initiated. The operation is assumed to start with the deployment of a heat shield to protect the temperature-sensitive electronics of the telescope imager. The mission is completed when the all the mirror tiles are installed in order to reach the primary mirror final aspects depicted in Fig. 3. A detailed sequence of assembly for such large telescope structure featuring such a robotic system can be found in [12].

To perform the assembly of such structure, the primary operations considered for the multi-arm installation robot are (1) re-localization to a new attachment point on the satellite, (2) transportation and (3) manipulation of hexagonal mirror tiles or ORU using its arm's or torso's SIs (Figs. 4, 5 and 6). Additional MAR operations, inherent to the modular concept of this robot, are extensively detailed in [12].

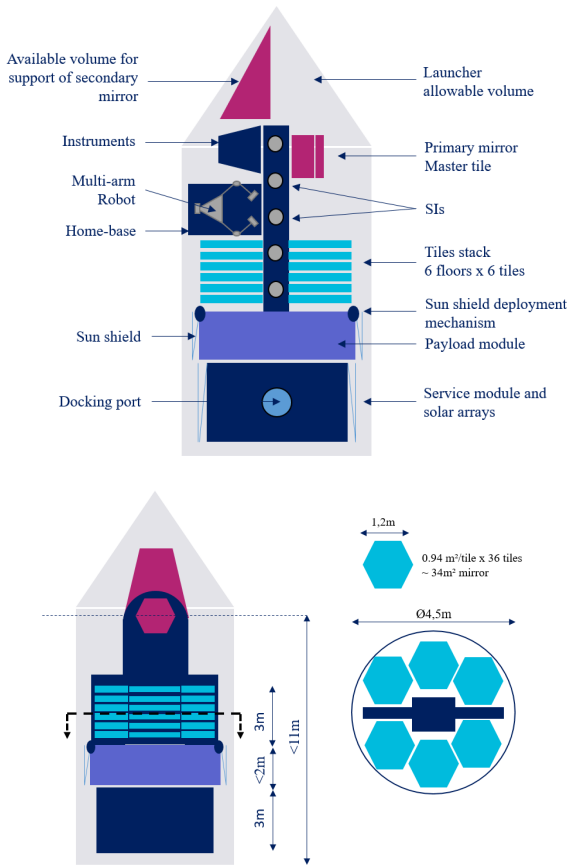


Figure 2. Launch configuration.

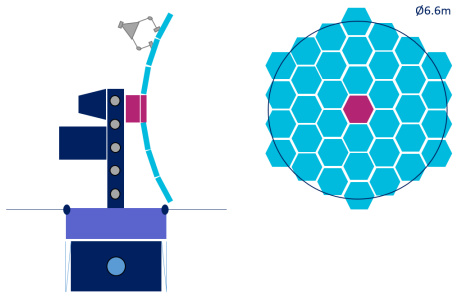


Figure 3. Final configuration of the telescope.

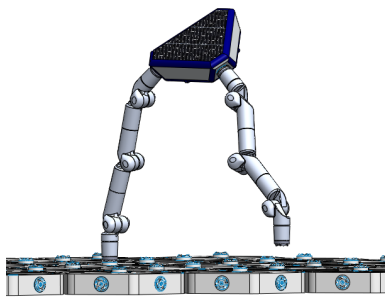


Figure 4. Artist representation of the walking operation.

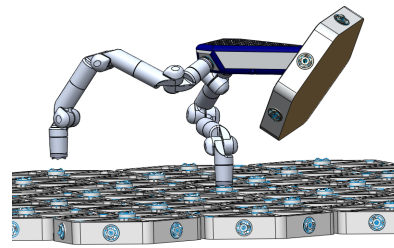


Figure 5. Artist representation of the transportation operation.

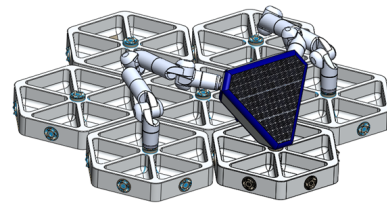


Figure 6. Artist representation of the manipulation operation.

3. Breadboard and demonstration scenario

For the purpose of the validation of the MIRROR concept, a realistic 1-g breadboard system has been developed. This testbed demonstrates the tasks that will be carried out by the multi-arm robot during the assembly of a space-based structure. This will be achieved by building a 1g adaptation of a section of the telescope as shown in Fig. 7.

The items comprising the breadboard have been carried out to meet MIRROR's operational and environmental requirements. To adapt the scenario to a 1g environment some adjustments have been made. Instead of a complex 3D structure the constituent items of the breadboard are laid out in a plane. The home based is attached directly to the mirror tiles and the mirror tiles themselves are flattened. This 2D structure also has the benefit of simplifying the gravity compensation mechanism.

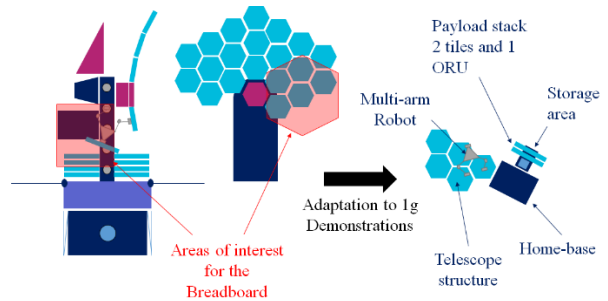


Figure 7. Adaptation of the space assembly task to the 1-g breadboard.

The proposed breadboard includes a home base, some pre-assembled mirror tiles and a storage area (or servicer) on which two tiles and an Orbit Replaceable Unit are stored. The overall structure, tiles and ORU are equipped with SIs. The number of mobile elements has been chosen to show the scope of assembly tasks faced when assembling hexagonal tiles, involving either one, two or three SIs simultaneously.

The demonstration scenario is structured as follows: initially the robot is located on its home base (including launch locks if this its first operation), as depicted in Fig. 8.



Figure 8. MIRROR Breadboard, initial position.

The robot disengages from its launch locks and grasp the first tile located on the storage area (Fig. 9).



Figure 9. MIRROR Breadboard, grasping tile1.

The robot walk along the structure and mirror tiles (Fig. 10).



Figure 10. MIRROR Breadboard, walking.

The robot installs the first tile at the dedicated location (Fig. 11).

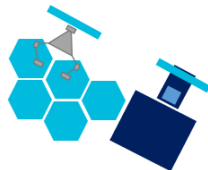


Figure 11. MIRROR Breadboard, installing tile1.

The robot walk back to the home base and grasp the second tile (Fig. 12).



Figure 12. MIRROR Breadboard, grasping tile2.

The robot walk along the structure and mirror tiles and install the second tile at the dedicated location (Fig. 13).



Figure 13. MIRROR Breadboard, positioning tile2.

The robot walk back to the home base and grasp the ORU (Fig. 14).

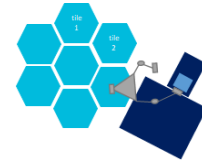


Figure 14. MIRROR Breadboard, grasping ORU.

The robot walk along the structure and mirror tiles and install the ORU at the dedicated location (on the spacecraft or on the mirror tile structure), as shown in Fig. 15.

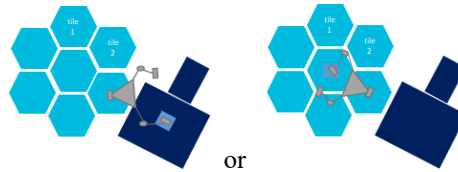


Figure 15. MIRROR Breadboard, positioning ORU.

Finally, the robot walk back to the home base (Fig. 16).

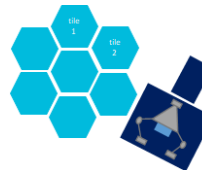


Figure 16. MIRROR Breadboard, final position.

4. Breadboard detailed design

Developed at TRL4, the MIRROR technological demonstrator, illustrated in Fig. 17, features a ground and a flight segment as follows:

- Flight segment:
 - The “Multi arm relocatable manipulator” (MAR) capable of grasping, releasing, and transporting payloads (mirror tiles and ORU). The MAR includes independent avionics to implement motion and to provide power to its actuator.
 - The “MIRROR testbed” provides the physical environment where the MAR system can demonstrate its functions in six degrees of freedom. The proposed MIRROR testbed includes a dummy spacecraft body, hexagonal telescope tiles and ORU equipped with SIs and a weight compensation device.
- Ground segment:
 - The “Monitoring and Control Station” (MCC) that allows users to supervise MAR’s tasks. This ground segment involves a programming interface linked with a simulator and a task/motion planner.
 - The “Electrical Ground Support Equipment” (EGSE) or power subsystem provides power to the Control Station.

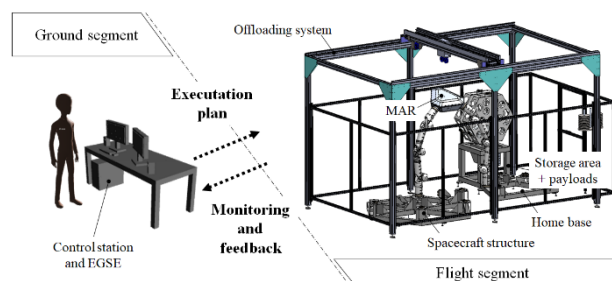


Figure 17. MIRROR's ground demonstrator concept.

4.1 Multi-arm robot

4.1.1 Mechatronics

In terms of kinematics, size, and functions, the MAR, shown in Fig. 18, is a ground equivalent modular robot of the flight concept [12]. It has two symmetrical anthropomorphic arms with seven degrees of freedom each and a torso, making up its three robotic subsystems. The robot's main body is its torso. Three

additional appendages (limbs or payloads) can be equipped with this mechanical hub, or it can be directly fastened to the spacecraft's frame. High-level information is transmitted to and from the connected modules via this central subsystem, which also supplies the necessary power. The torso also has vision and perception devices for monitoring, as well as an energy storage pack in case other energy sources are unavailable. Robotic arms are limbs that can function as either arms or legs, depending on the robot's desired configuration. Following the results of an appropriate locomotion or manipulation planning stage, they can be used to move the robot or manipulate payloads. The torso and robotic arms are functionally independent robotic subsystems that can be linked by SIs (see Fig. 19). The MAR's modular design aims to simplify the various robotic appendages and offers a variety of robotic configurations that increase the scope of possible operations and offer an inherent system redundancy that lowers mission risk overall. To accomplish this, a locomotion controller based on passivity has been created to carry out all MAR operations for the morphologies mentioned above. In the presence of the SI constraints, the controller's Cartesian impedance characteristics enable a compliant behaviour. Additional technical details about the MAR breadboard design can be found in [13].

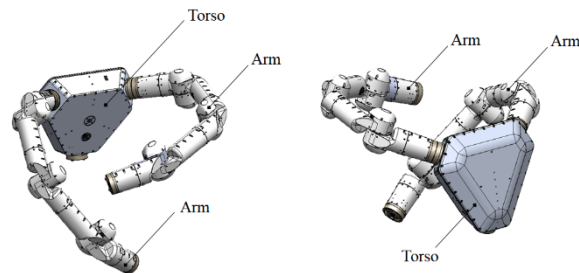


Figure 18. Detailed design of the MAR.

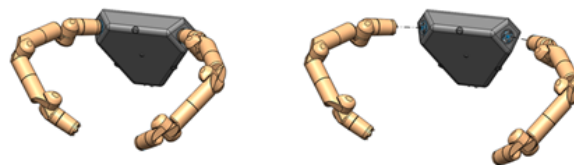


Figure 19. MAR system modular assembly: torso (grey) and robotic manipulator (orange).

4.1.2 Software

The Multi Arm Robot (MAR) control system includes three layers, which are described as follows:

- The low-level controller layer that controls each robot joint drive using an EtherCAT communication stack.

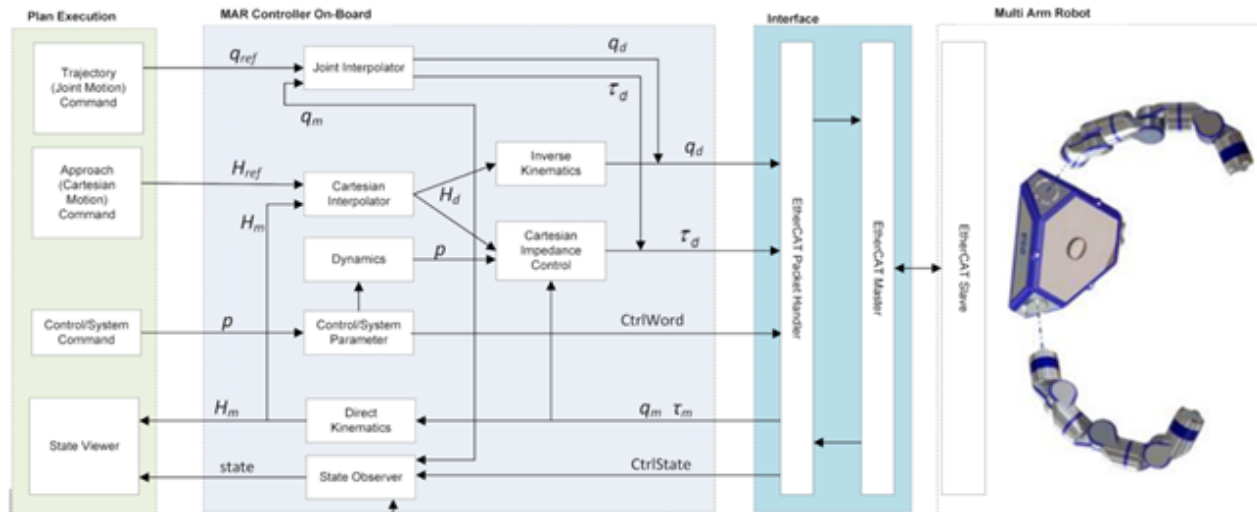


Figure 20. Control software architecture.

- The control-software layer that sets position or torque commands based on advanced control techniques (such as the Cartesian Impedance Controller) and enables or disables MAR motion.
- The path planning layer, which generates a series of operations representing the motion of the manipulator system, system configuration applied to carry out the desired operation, and commanding of the SI.

Fig. 20 depicts every component needed to control the MAR system, from low-level control to high-level control.

The planning interface uses the description of the task that the robot must complete in order to provide the desired trajectories to the control-software. It receives the current state from the MAR via the MAR controller on the OBC. These paths ensure that the task can be completed while adhering to motion restrictions, such as singularity and collision avoidance. Finally, for monitoring purposes and to identify the need for re-planning, the planner also receives operation status and flags from the control software.

Each joint drive has a low-level control program that runs on the SCU. The motor drive setpoint controller and an implementation of the EtherCAT communication interface are present, and they are both controlled by the control-software layer for each joint individually. Torque and position are the two modes of operation for the low-level controller. Each mode corresponds to the signals, such as desired torques or positions, sent by the control-software layer. The low-level controllers ensure that the motor drive will receive the desired torque or position values, depending on the control mode. The

low-level controllers must operate at a control frequency greater than the high-level control frequency for this cascaded control structure to be effective. For the control-software layer, typical values are 1 kHz, and for the low-level controller, they are 3 kHz.

4.1.3 Control

The architecture in Fig. 20 summarizes the on-board controller of the MAR system within the light-blue area. Apart from the standard elements needed for controlling the robot used in position control (e.g. joint interpolator, inverse kinematics, etc.), an advanced Cartesian impedance control was designed for the MAR system. In general, impedance controllers for space manipulators are effective in dealing with contacts, see e.g. [14], [15] and [17]. This controller is based on joint torques commands, which ensures stable behavior during the contact. Since the MAR system needs to perform contact-oriented tasks, an impedance controller is also considered in the design. The details of this controller are reported in [16] and it will be summarized as follows along with preliminary results.

The developed controller uses the constrained dynamics in the analysis to derive a unified joint torque control law for all the considered operations and morphologies. In particular, the designed impedance controller ensures passivity during external contacts (e.g. latching with the SIs), which provides a measure of stability against perturbations. The SI latching points of the MAR system are modelled as bilateral constraints, and the number of constraints is given by the number of latching points.

The Cartesian control law is shown in the yellow block of Fig. 21. It requires the kinematic computations, which is performed in the blue box while using the MAR

plant joint measurements (q). The plant can be the one of the 1-arm, 1-arm + torso, 2-arm or torso system. The overall Cartesian impedance control law is given as:

$$\hat{\tau} = \tau_{ff}(g^*_d) + \tau_n(q) + \tau_{fb} + \tau_{jl}(q),$$

where τ_{ff} are the feed-forward terms for the trajectory tracking of the desired pose, g^*_d , τ_n is the null-space control torque and τ_{fb} is the feedback part, which is written as,

$$\tau_{fb} = T(q)^T \left(-\gamma - DT(q) \begin{bmatrix} V_b \\ \dot{q} \end{bmatrix} \right).$$

D is a positive-definite matrix of the damping gains, $T(q)$ is the Jacobian and γ consists of the total wrench(es) due to the proportional action corresponding to the potential ϕ , which provides the P-control (proportional) term. V_b is the body velocity corresponding to the pose g_b and \dot{q} is the joint velocity. For safety in the operation, a torque component, τ_{jl} , is added in the control. This prevents the violation of the hardware limit of the joints of the MAR system and this is designed using a repulsive spring-damper behaviour.

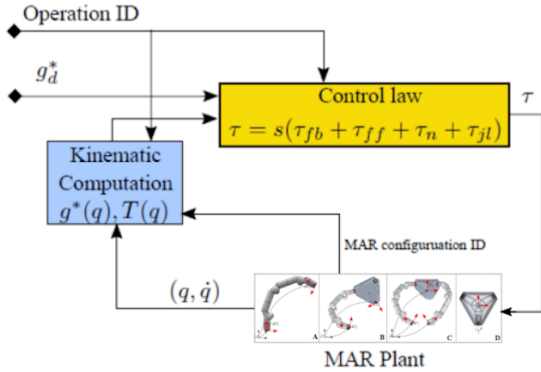


Figure 21. Control Architecture.

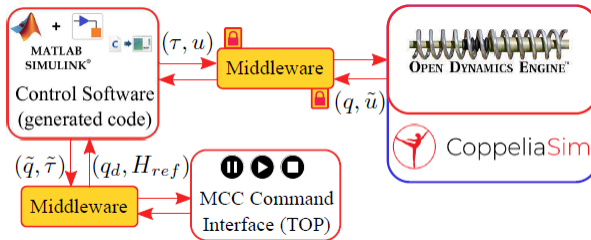


Figure 22. Control Software Integration.

For control prototyping, the co-simulation framework from [16] was extended further to accommodate the avionics architecture of the MAR system (Fig. 20) and the MIRROR's ground demonstrator (Fig. 17). In particular, the new co-

simulation framework is shown in Fig. 22 and it was extended to:

- generate control software code for deployment in the flight segment.
- include the MCC Command Interface (TOP, Task Oriented Programming) for ground segment.

The TOP (Task Oriented Programming, see [18] for details) system enables generation and initialization of robot actions at different levels of abstraction:

1. Elementary Operations (ElemOp)
2. Operations (Op)
3. Tasks (Task)

The ElemOp layer represents all the actions available at joint or Cartesian level for each actuator. At the Operation layer, a sequence of ElemOps are generated, which activates an autonomous action, e.g. approach a mirror tile. ElemOps for simultaneous activation of actuators at the joint or cartesian level are combined for concurrent execution. Cartesian movements are performed relative to the selected object, e.g. a mirror tile. At the Task layer, a sequence of Operations can be generated, e.g. for walking operation.

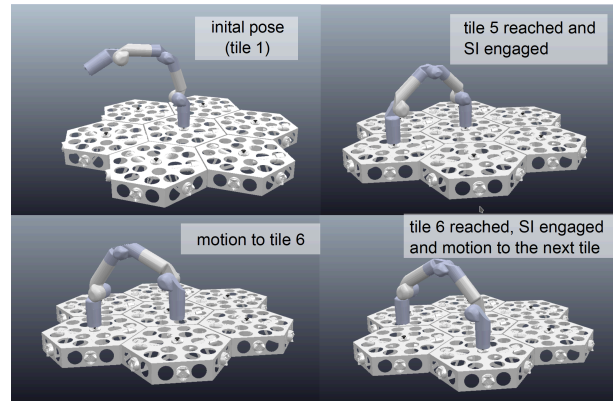


Figure 23. Example of walking operation for 1 arm system.

An example of the walking operation for the one arm system using the proposed co-simulation framework is shown in Fig. 23. The manipulator moves from an initial configuration (tile 1) to another tile (tile 5) using the Cartesian impedance controller. After reaching the tile 5, the end-effector gets attached and the feedback computation is changed. In such a way, the manipulator can move towards the second tile (tile 6). Fig. 24 shows the end-effector error in position and orientation during the described motion. At $t=0$, the arm has an error in position and orientation that converges to zero at $t=27s$, consequentially the SI is engaged to lock the end-effector to the first tile. A new pose is given as

input to the controller at $t=27.1s$ to reach the second tile, which occurs at $t=50s$. The same operation is repeated at $t=50.1s$. The increase in error, at $t=27.1s$ ($t=50s$), marks a new step, i.e. a new desired pose is set for the unconstrained end-effector where the system moves. The results show the effectiveness of the developed unified controller in performing the walking task and more details can be found in [16].

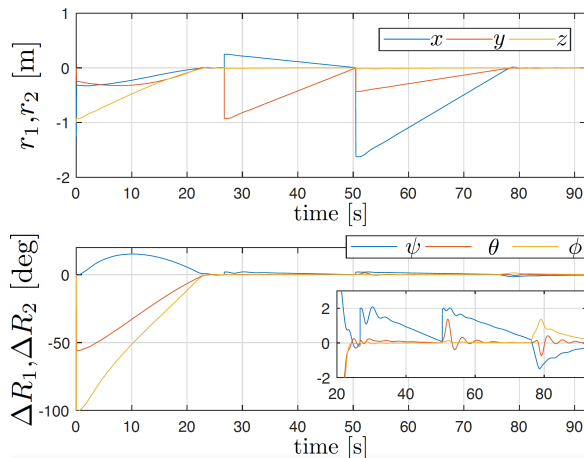


Figure 24. Error in position and orientation during the walking operation.

4.2 Testbed design

4.2.1 Dummy spacecraft

The dummy spacecraft, depicted in Fig. 25, is composed of a home base, storage area and a telescope structure.

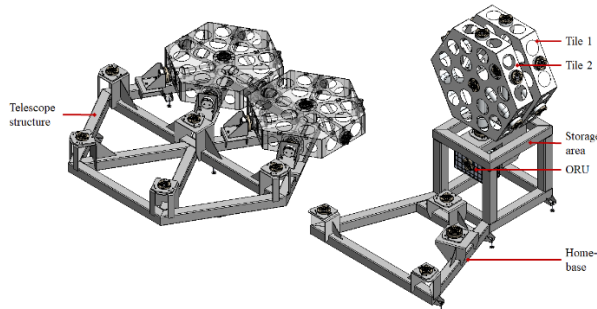


Figure 25. Overview of the MIRROR dummy spacecraft.

The home is a platform that hosts the robot when not used and provides an excess to the payloads and to the telescope structure. The home base is equipped with an ORU compartment for hosting electronic devices (for example). The storage area is a structure on which the payloads are initially mounted. The telescope structure is a fixed structure involving prepositioned dummy tiles, allowing the robot to move along it.

The different structures of the dummy spacecraft

feature SIs as illustrated in Figs. 26 and 27. The location and type of SIs has been careful chosen to reduce the complexity of the testbed and to provide a relevant workspace to the robot in order to illustrate and perform its scope of operations.

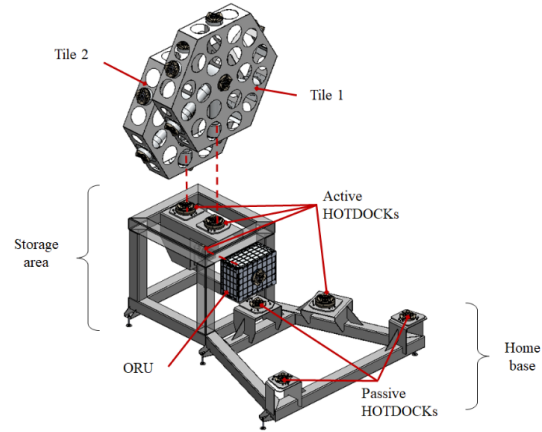


Figure 26. Detailed design of the home base and storage area.

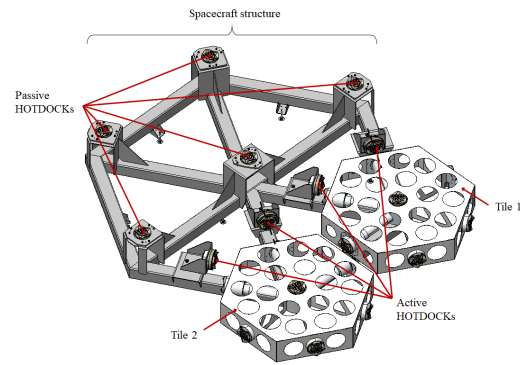


Figure 27. Detailed design of the telescope structure.

4.2.2 Payloads

The dummy payloads are composed of two hexagonal mirror tiles and one parallelepiped ORU. Each payload features SIs as illustrated in Figs. 28 and 29. The mirror tiles are 1.2m large (corner to corner) and weigh 10kg. The ORU features a 275x390x190mm aluminum structure and weighs 5kg.

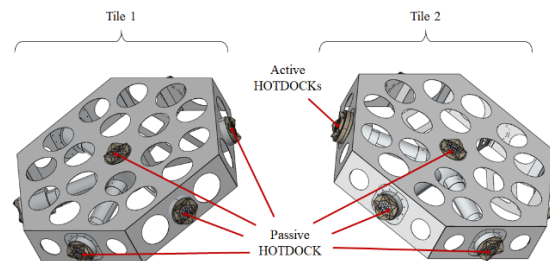


Figure 28. Detailed design of the mobile tiles.

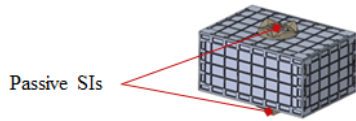


Figure 29. Detailed design of the ORU.

4.2.3 Weight compensation device

The weight compensation device of MIRROR is a passive gantry crane mechanism with a passive rolling bridge equipped with trolleys to support the system along the X and Y directions (see Figs. 30, 31 and 32). The Z-axis load vector is supported by a cable system involving pulleys and counterweights. This configuration allows for moving in X and Y directions without inducing a Z motion. Thus, only a translation of the MAR in the Z direction influences the height of the counter mass. This structure is composed of aluminium profiles and measures 3mx5mx3m.

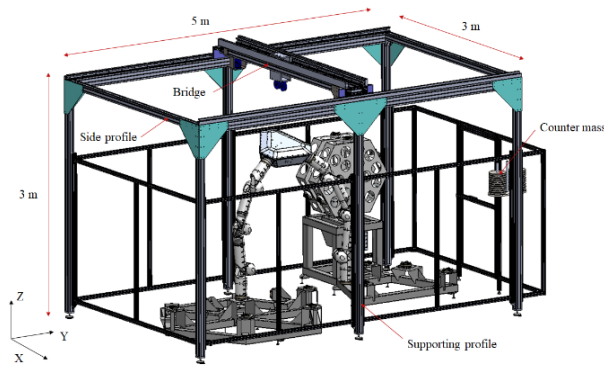


Figure 30. Gantry crane system with testbed.



Figure 31. Possible motions of the offloaded object.

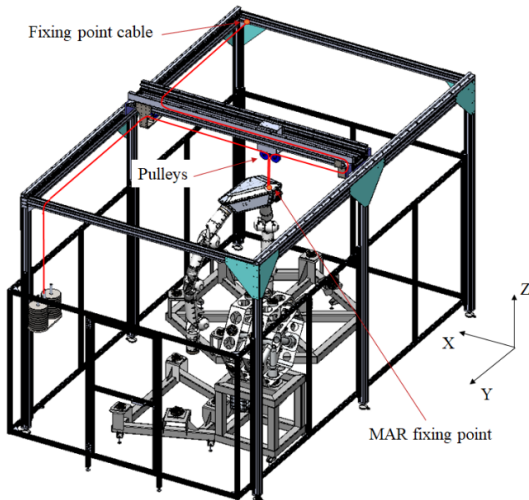


Figure 32. Cable routing along the gantry crane.

4.3 Ground segments

The ground segment of this testbed is composed of a programming and control station and an EGSE. The programming and control station monitors and controls the demo setup. It will run on a standard computer (x86), with Linux OS (Ubuntu 18.04 or above), running the Console/Service. The EGSE provides the electrical and data components required to operate the system. It mainly involves a power supply with two channels (one dedicated to power the robot, the second one dedicated to power the testbed devices), a CPDU, two CAN networks (for controlling the testbed interconnects and for communicating high-level commands to the MAR) and a wireless router for remote connection with the MAR OBC.

5. MIRROR breadboard preliminary integration

The MIRROR breadboard is presently under integration and testing. Fig. 33 illustrates the MAR and ORU assemblies while Fig. 34 depicted the weight compensation device. Testing and final results are foreseen by Q1 2023.

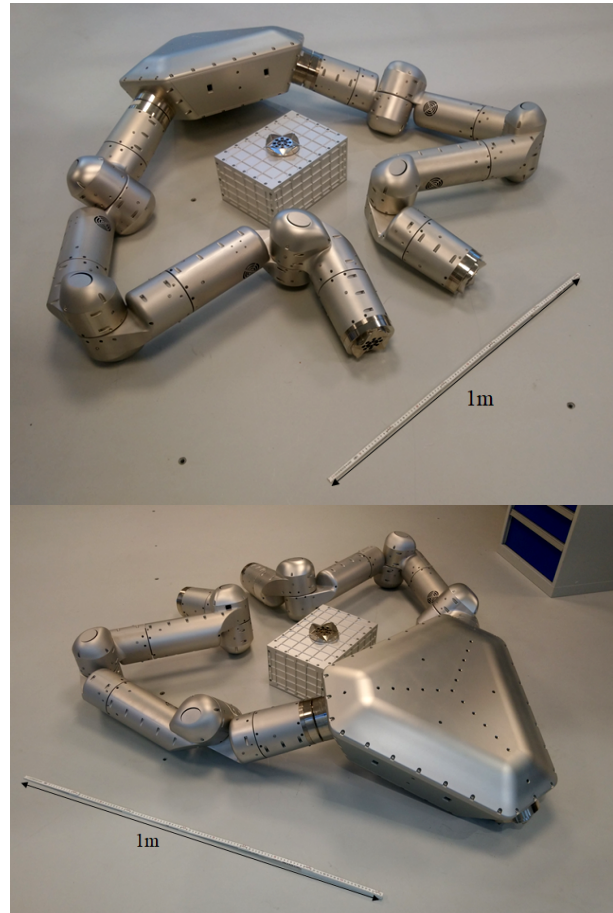


Figure 33. MAR ground demonstrator and ORU.



Figure 34. MIRROR's weight compensation device.

6. Conclusions and Perspectives

This paper describes the ground demonstrator (TRL4) design and preliminary integration for a multi-arm robot dedicated to on-orbit large assembly, performed in the scope of the ESA TRP MIRROR project.

This technological ground breadboard, derived from the MIRROR mission concept of operations, aims to demonstrate the entire scope of operations of this novel modular installation robot in a representative environment.

Future work will focus on achieving the entire integration of the breadboard as well as testing the MAR within the MIRROR demonstrator. In parallel to this activity, the use of such modular robotic systems is assessed in the scope of in-orbit very large structure assembly applied to space solar power plant through the ESA OSIP SKYBEAM study.

Acknowledgements

This study is funded by ESA in the framework of the Technology Research program (contract No. 4000132220/20/NL/RA) entitled "Multi-arm Installation Robot for Readyng ORUS and Reflectors (MIRROR)".

References

[1] M. Rognant, et al. (2019). Autonomous assembly of large structures in space: a technology review. EUCASS 2019, Madrid, 2019.

[2] R. Mukherjee, et al. (2019). The future of space astronomy will be built: Results from the in-space astronomical telescope (isat) assembly design study. 70th International Astronautical Congress (IAC), Washington D.C., 2019.

[3] M.A. Post, et al. (2021). Modularity for the future in space robotics: A review. *Acta Astronautica*, 2021, vol. 189, p. 530-547.

[4] P. Letier, et al. (2020). HOTDOCK: Design and Validation of a New Generation of Standard Robotic Interface for On-Orbit Servicing. 71th International Astronautical Congress (IAC), The CyberSpace Edition, 2020.

[5] MM. Arancón, et al. (2017). "ESROCOS: a robotic operating system for space and terrestrial applications." 14th Symposium on Advanced Space Technologies in Robotics and Automation (ASTRA). 2017.

[6] J. Vinals, et al. (2020). "Standard Interface for Robotic Manipulation (SIROM): SRC H2020 OG5 Final Results-Future Upgrades and Applications." i-SAIRAS 2020.

[7] M.A. Roa, et al. (2022). PULSAR: Testing the technologies for on-orbit assembly of a large telescope. In 16th ESA Workshop on Advanced Space Technologies for Robotics and Automation, ASTRA, Noordwijk, 2022.

[8] P. Letier, et al. (2019). MOSAR: Modular Spacecraft Assembly and Reconfiguration Demonstrator, ASTRA, 15th Symposium on Advanced Space Technologies in Robotics and Automation, Noordwijk, Netherlands, 2019.

[9] M. Deremetz, et al. (2020). MOSAR-WM: A relocatable robotic arm demonstrator for future on-orbit applications. In 71th International Astronautical Congress (IAC), The CyberSpace Edition, 2020.

[10] P. Schoonejans, et al. (2004). "Eurobot: EVA-assistant robot for ISS, Moon and Mars." Proceedings of 8th ESA Workshop on Advanced Space Technologies for Robotics and Automation, ASTRA, Noordwijk. 2004.

[11] A. Rusconi, et al. (2009). Dexarm engineering model development and test. In 10th ESA Workshop on Advanced Space Technologies for Robotics and Automation, ASTRA, Noordwijk, 2009.

[12] M. Deremetz, et al. (2021). Concept of operations and preliminary design of a modular multi-arm robot using standard interconnects for on-orbit large assembly. In 72st International Astronautical Congress (IAC), Dubai, 2021.

- [13] M. Deremetz, et al. (2022). Demonstrator design of a modular multi-arm robot for on-orbit large telescope assembly. In 16th ESA Workshop on Advanced Space Technologies for Robotics and Automation, ASTRA, Noordwijk, 2022.
- [14] De Stefano, M., et al. (2019). Multi-rate Tracking Control for a Space Robot on a Controlled Satellite: a Passivity-based Strategy, IEEE Robotics and Automation Letters (RA-L), pp. 1319-1326, 10.1109/LRA.2019.2895420, 2019.
- [15] Mishra, H., et al. (2020). A geometric controller for fully-actuated robotic capture of a tumbling target. In American Control Conference (ACC), 2150–2157.
- [16] Mishra, H., et al. (2022). Dynamics and Control of a Reconfigurable Multi-Arm Robot for In-Orbit Assembly. In 2022 Vienna International Conference on Mathematical Modelling (MATHMOD), Vienna, July 2022.
- [17] De Stefano M., et al. (2015). On- ground experimental verification of a torque controlled free-floating robot. 13th Symposium on Advanced Space Technologies in Robotics and Automation 2015 (ASTRA), ESA/ESTEC.
- [18] B. Brunner, et al. (1994). "Task directed programming of sensor based robots," Proceedings of IEEE/RSJ International Conference on Intelligent Robots and Systems (IROS'94), 1994, pp. 1080-1087 vol.2.